A Chandra Legacy Observation of the LMC SNR N132D

P. P. Plucinsky (Harvard-Smithsonian Center for Astrophysics) on behalf of the N132D Legacy Team

Abstract

N132D is the most X-ray luminous supernova remnant (SNR) in the Local Group. Given its location in the Large Magellanic Cloud, it is a prime target for detailed X-ray studies with the Chandra X-ray Observatory. The existing 87 ks Chandra observation of N132D has revealed the complicated spatial and spectral structure of this SNR, but the depth of this observation limits the spatial scale on which detailed spectroscopy may be performed. We successfully proposed for a Chandra legacy observation (900 ks) of N132D that will permit anunprecedented look at the spatial distribution of iron and other heavy elements in the ejecta from this prototypical core-collapse supernova. Combined with supporting multiwavelength data (from radio to gamma rays), these data will inform many areas of active research, including late stages of massive star evolution, explosion mechanisms and dynamics, and physical mechanisms for the interaction of shocks with molecular clouds and cavities. Observations such as this one provide a unique and important way to constrain models of massive stars and the supernovae they produce. Our observational program has begun and has acquired 353 ks of the full exposure of 900 ks. We will present preliminary results from the observations performed to date.

X-ray Image Analysis

- Table 1 lists the archival observations and our new observations
- Figure 1 displays the image in the 0.35-8.0 keV band from the archival observations
- Figure 2 displays a three color image from a merged data set of the archival and our new observations
- Figures 3a-d show the narrow bands images from the merged data in the following bands O-VIII Ly-α (0.60-0.73 keV), Ne IX Heα triplet & Ne X Ly-α (0.80-1.10 keV), Si XIII Heα triplet(1.75-1.95 keV), and S XV Heα triplet (2.35-2.55 keV)
- Figure 4 shows the raw counts (LEFT) and smoothed counts (RIGHT) in the 6.5-6.9 keV band with the total X-ray intensity contours overplotted.

N132D

N132D is the brightest X-ray SNR in the LMC, with a luminosity of L_x(0.3-10.0 keV)~1.0x10^{38} ergs/s. N132D was classified as an O-rich remnant based on optical spectra (Lasker 1978). The remnant has a complicated morphology in X-rays with many bright filaments which appear along the line-of-sight to the interior of the remnant and several faint protrusions ahead of the brightest parts of the shock. The southwestern part of the remnant appears to have a semi-circular shell but the northeastern part of the remnant has a fragmented and decidedly non-spherical structure. A dense CO cloud has been mapped just to the south of the remnant (Banas et al. 1997, Sano et al. 2015). The X-ray, optical, and IR morphology are consistent with a remnant expanding into a cavity, and the bright shell emission indicates an interaction between the main blast wave and the cavity wall in the south (Hughes 1987 and Sharda et al. 2019). Morse et al. (1996) estimated an age of ~3,000 yr based on the expansion of the O-rich knots. HST Faint Object Spectrograph (FOS) showed lines of C, O, Ne, & Mg but no evidence of Si, S, Ca, & Ar. Blair et al. (2000) suggested that the progenitor may have had an O-rich mantle which did not mix with the innermost ejecta layers. France et al. (2009) claim detection of weak Si IV emission, in addition to C and O, from an HST Cosmic Origins Spectrograph (COS) spectrum. Early XMM results based on only 23 ks of data (Behar et al. 2001) show a centrally concentrated morphology for the Fe-K emission, while the O-K, Ne-K and Fe-L emission trace the outer bright parts of the shell. Vogt & Dopita (2011) constructed a 3D map of the [O III] filaments to show that the O ejecta form a ring 12 pc in diameter inclined ~25 degrees from the line of sight and estimated an age of 2,500 yr. Borkowski et al. (2007) used the high-resolution image from Chandra to conclude that some of the O emission seen in X-rays was co-spatial with some of the O filaments seen in the optical.

Table 1: Archival Data and Cycle 20 Data

OBSID	Date	Exp(ks)
5532	2006-01-09	44.6
7259	2006-01-10	24.9
7266	2006-01-15	19.9

Archival == 89 ks
Cycle 20 == 353 ks

OBSID	Date	Exp(ks)
21362	2019-03-27	34.4
21363	2019-08-27	46.5
21364	2019-09-01	21.0
22687	2019-09-02	34.8
22094	2019-09-10	36.6
21687	2019-09-11	25.0
22841	2019-09-12	36.9
22853	2019-09-22	20.0
22740	2019-09-26	20.0
22858	2019-09-27	20.0
22859	2019-09-28	20.0
21881	2019-10-04	23.5
22860	2019-10-06	18.0

N132D Legacy Team

Aya Bamba (U. of Tokyo), William Blair (JHU), Daniel Castro (SAO), Adam Foster (SAO), Kristen Garofali (U. of Arkansas), Terrance Gaetz (SAO), Kosuke Hatauchi (U. of Tokyo), Vinay Kashyap (SAO), Charles Law (Harvard), Dan Milisavljevic (Purdue), Eric Miller (MIT Kavli Institute), Dan Patnaude (SAO), Paul Plucinsky (SAO), Hidetoshi Sano (U. of Nagoya), Manami Sasaki (U. Erlangen-Nuremberg), Piyush Sharda (Australian National U.), Ben Williams (U. of Washington), Brian Williams (GSFC), Hiroya Yamaguchi (ISAS)

Shell Spectral Fits to Archival Data

We exploited the superb imaging capabilities of Chandra to extract spectra from the outer shell (Sharda et al. 2019) which should be dominated by interstellar medium (ISM) material swept up by the forward shock. These twenty regions are shown in Figure 5. The spectra were fit with a vpshock model and two components for the absorption (one Galactic and one for the LMC). A typical spectra for region #6 is shown in Figure 6. For most of the regions, a single vpshock model provides an adequate fit. For three regions, the fit is significantly improved with the addition of a vnei component. Figure 7 shows the spectral fit to region #3 with a combined vpshock+vnei model. It is possible that for these three regions some ejecta emission is mixing with the swept-up ISM material. We used the regions that were adequately fit by a single vpshock model to determine the abundances of O, Ne, Mg, Si, S, & Fe in the local ISM.

Inner Region Spectral Fits to Archival Data

We extracted spectra from the regions labelled “e1” and “f1” to “f5” in Figure 5. The e1 region overlaps with a region that shows enhanced abundances in the optical spectra. The f1-f5 regions show enhanced Fe-K emission in the Chandra data. The e1 spectra was fit with a vnei+vpshock model (Figure 8). The vpshock model is intended to model the shell emission along the line of sight to this region and the vnei model is intended to represent the ejecta emission. The O, Ne, Mg, Si, and Fe are all enhanced with respect to LMC abundances. Assuming that this spectral model is representative of pure ejecta, we calculated the ratios of these elements and compared them to the nucleosynthesis models in Sukhbold et al. (2016). We fit the the f1-f5 regions with a vpshock+vnei+vrnei model. The fit to region f3 is shown in Figure 9. Hitomi Collaboration (2018) and Bamba (2018) have recently claimed evidence of a recombining plasma. We derived the Fe/Si ratio from these fits as suggested in Katsuda et al. (2018). Combining the results of the abundance measurements, the ratios are most consistent with a progenitor mass of 16 +\- 6$M_\odot$.

Figure 1: Chandra 0.35-8.0 keV band image

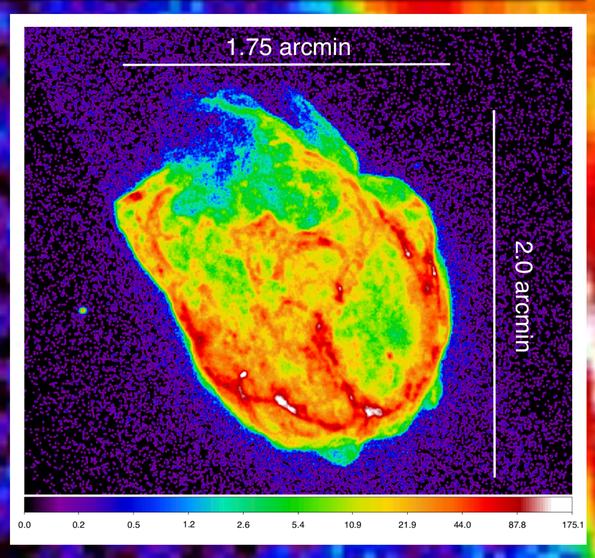

Figure 2: Three Color from merged data

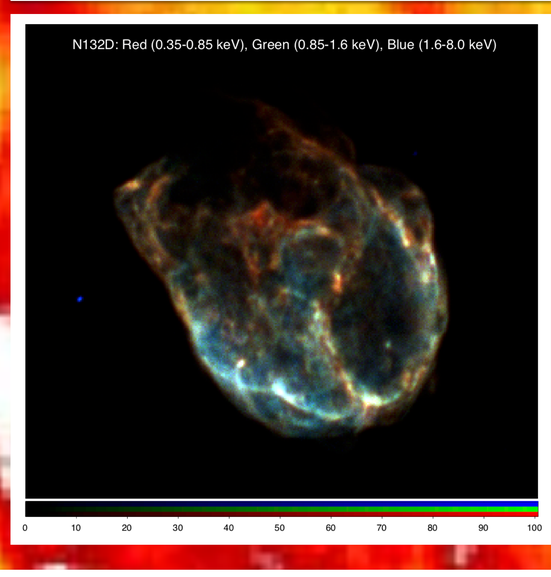

Figure 3: Chandra narrow band images: a) O-VIII Ly-α, b) Ne IX Heα & Ne X Ly-α, c) Si XIII Heα d) S XV Heα

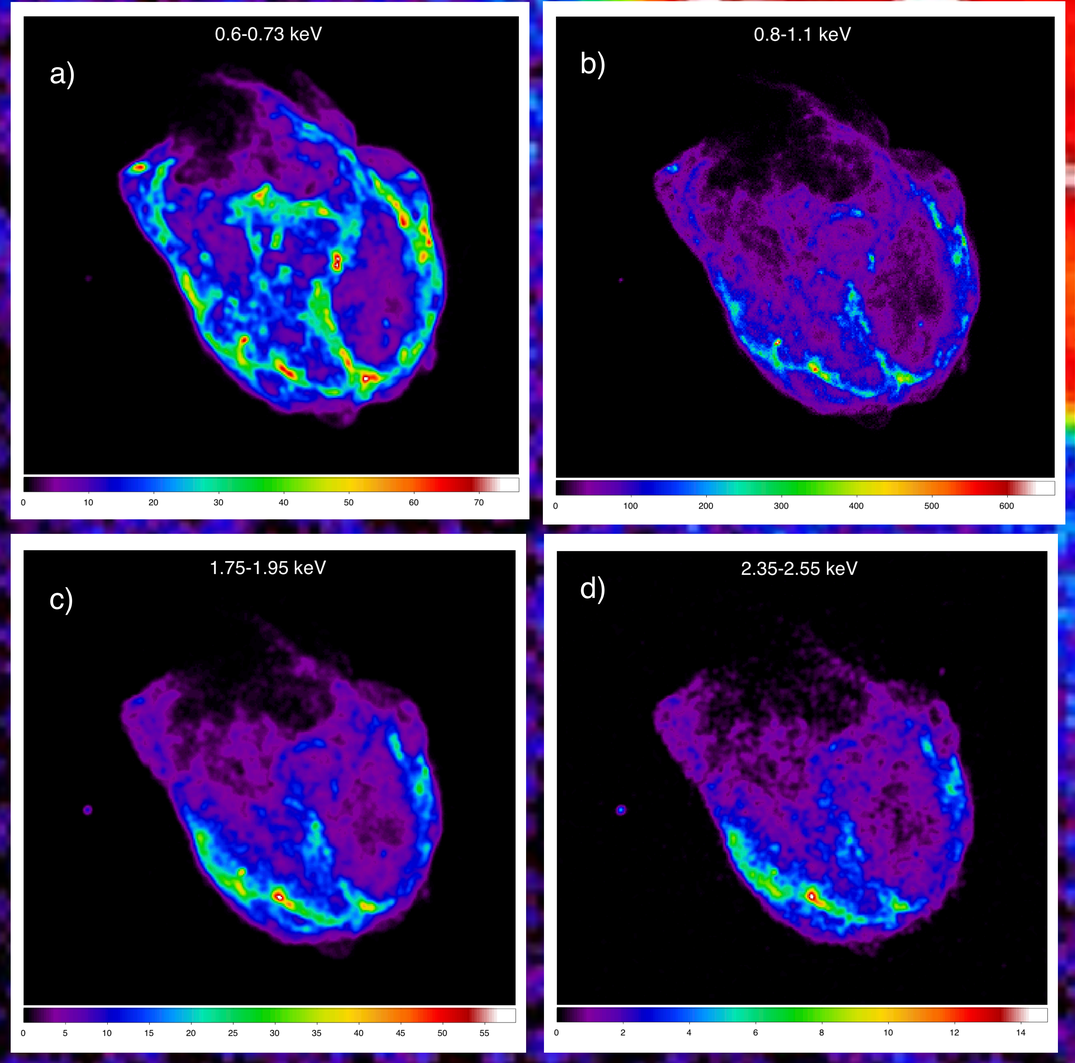

Figure 4: Raw and smoothed counts in the Fe K region.

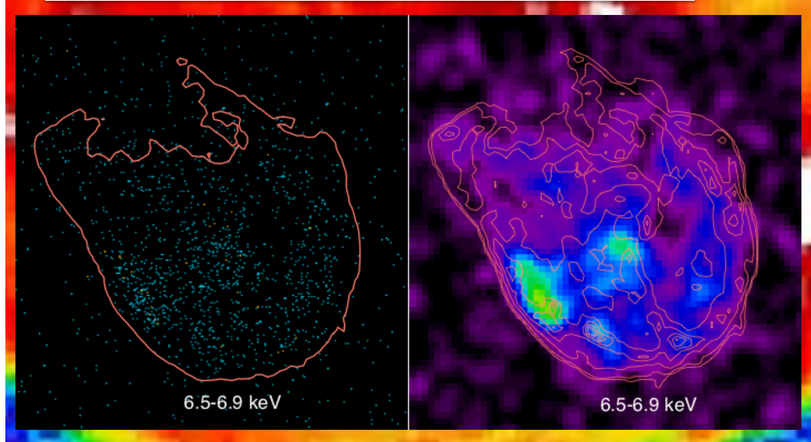

Figure 5: Extraction Regions from

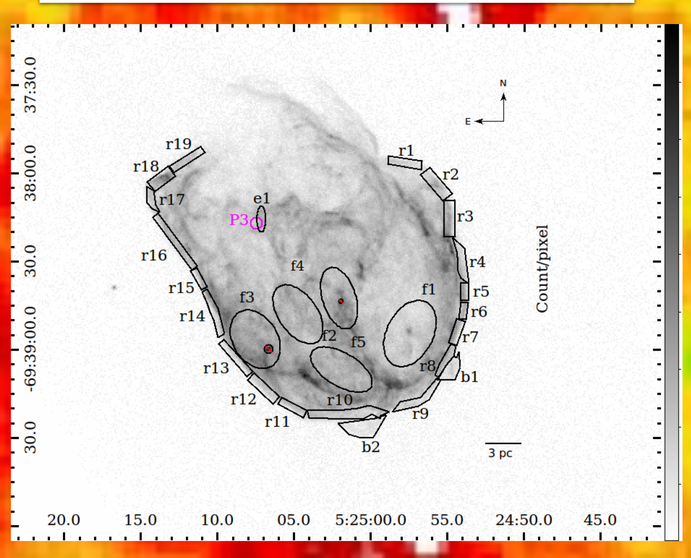

Figure 6: RIM region #6 vpshock fit

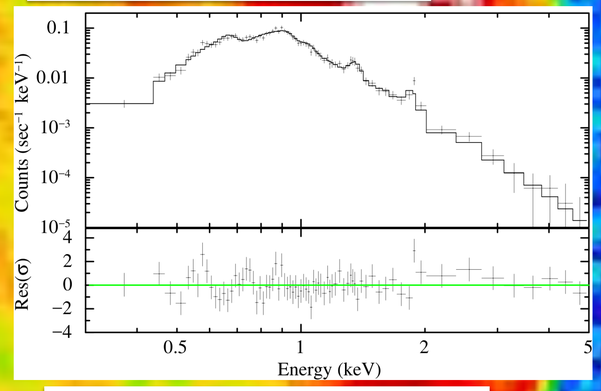

Figure 7: RIM region #3 vpshock+vnei fit

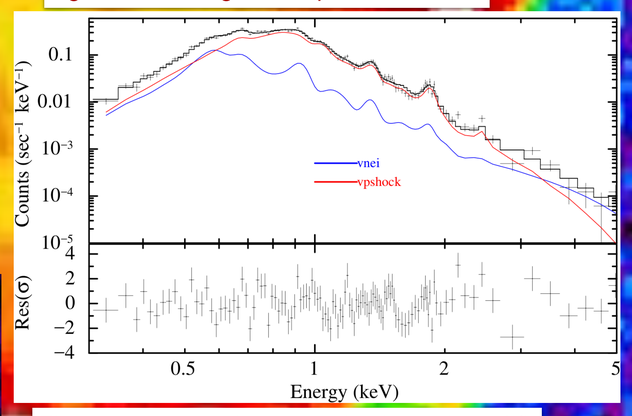

Figure 8: Inner region e1 vpshock+vnei+vnei fit

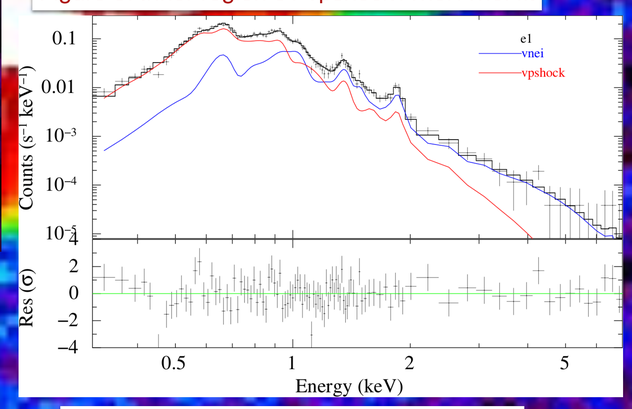

Figure 9: region f3 vpshock+vnei+vrnei fit

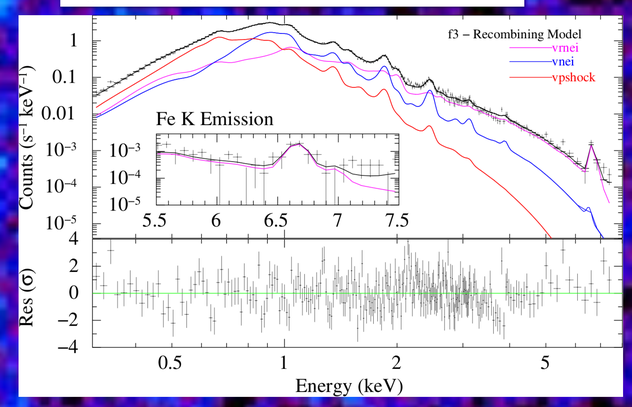

References:

Banas, K.R. et al. 1997, ApJ, 480, 60
Bamba, A. et al. 2018, ApJ, 854, 71
Behar, E. et al. 2001, A&A, 365, L242
Blair, W.P. et al. 2000, ApJ, 537, 667
Borkowski, K.J. et al. 2007, ApJ, 671, L45
France, K. et al. 2009, ApJ, 707, L27
Hitomi Collaboration, 2018, PASJ, 70, 16
Hughes, J.P. 1987, ApJ, 314, 103
Katsuda, S. et al. 2018, ApJ, 863, 127
Lasker, B.M. 1978, ApJ, 223, 109
Morse, J.A. et al. 1996, AJ, 112, 509
Sano, H. et al. 2015, ASP Conference Series, 499, 257
Sharda, P. et al. 2019, ApJ, submitted
Sukhbold, T. 2016, ApJ, 821, 38
Vogt, F., & Dopita, M.A. 2011, APSS, 331, 521